Peng *et al. Chem Synth* 2022;2:15
DOI: 10.20517/cs.2022.15

Chemical Synthesis

Research Article

Open Access

Customization of functional MOFs by a modular design strategy for target applications

Yaguang Peng[1,2], Qiang Tan[1], Hongliang Huang[1,*], Qinggong Zhu[2], Xinchen Kang[2,3,*], Chongli Zhong[1], Buxing Han[2,3,*]

[1]State Key Laboratory of Separation Membranes and Membrane Processes, School of Chemical Engineering and Technology, Tiangong University, Tianjin 300387, China.
[2]Beijing National Laboratory for Molecular Sciences, Key Laboratory of Colloid, Interface and Thermodynamics, CAS Research/Education Center for Excellence in Molecular Sciences, Institute of Chemistry, Chinese Academy of Sciences, Beijing 100190, China.
[3]School of Chemistry, University of Chinese Academy of Sciences, Beijing 100049, China.

[*]**Correspondence to:** Prof./Dr. Hongliang Huang, State Key Laboratory of Separation Membranes and Membrane Processes, School of Chemical Engineering and Technology, Tiangong University, No. 399 BinShuiXi Road, Tianjin 300387, China. E-mail: huanghongliang@tiangong.edu.cn; Prof./Dr. Xinchen Kang, Beijing National Laboratory for Molecular Sciences, Key Laboratory of Colloid, Interface and Thermodynamics, CAS Research/Education Center for Excellence in Molecular Sciences, Institute of Chemistry, Chinese Academy of Sciences, No. 2 Zhongguancun North First Street, Beijing 100190, China. E-mail: kangxinchen@iccas.ac.cn; Prof./Dr. Buxing Han, Beijing National Laboratory for Molecular Sciences, Key Laboratory of Colloid, Interface and Thermodynamics, CAS Research/Education Center for Excellence in Molecular Sciences, Institute of Chemistry, Chinese Academy of Sciences, No. 2 Zhongguancun North First Street, Beijing 100190, China. E-mail: hanbx@iccas.ac.cn

How to cite this article: Peng Y, Tan Q, Huang H, Zhu Q, Kang X, Zhong C, Han B. Customization of functional MOFs by a modular design strategy for target applications. *Chem Synth* 2022;2:15. https://dx.doi.org/10.20517/cs.2022.15

Received: 13 Jun 2022 **First Decision:** 8 Jul 2022 **Revised:** 20 Jul 2022 **Accepted:** 21 Jul 2022 **Published:** 28 Jul 2022

Academic Editors: Bao-Lian Su, Teng Ben **Copy Editor:** Peng-Juan Wen **Production Editor:** Peng-Juan Wen

Abstract

Herein, we propose a versatile "functional modular assembly" strategy for customizing MOFs that allows installing the desired functional unit into a host material. The functional unit could be switched according to different applications. MOF-808, a highly stable Zr-MOF containing dangling formate groups, was selected as a host material for demonstration. Functional molecules with carboxyl connectors can be directly inserted into MOF-808 to form functional modular MOFs (FM-MOFs) through single substitution, while for those without carboxyl connectors, a pre-designed convertor was grafted firstly followed by the functional molecules in a stepwise manner. A series of tailor-made FM-MOFs were generated and show excellent performance toward different applications, such as adsorption, catalysis, fluorescent sensing, electrochemistry, and the control of surface wettability. On the other hand, the functional units on the FM-MOFs can switch freely and completely via full interconversion, as well as partly to construct multivariate MOFs (MTV-MOFs). Therefore, this strategy provides a

benchmark for rapid customization of functional MOFs for diverse applications that can realize the rapid modular design of materials.

Keywords: Metal-organic frameworks, functionality, modular design strategy, customization

INTRODUCTION

Porous materials have been attracting intense attention owing to their wide range of potential applications[1,2]. Rational design and functional targeting synthesis of porous materials on demand by the introduction of functional groups or molecules are essential for practical application[3,4]. It is relatively difficult to insert and modify functional groups in the structures of conventional porous solids such as zeolites and activated carbons, especially at the molecular level, whereas metal-organic frameworks (MOFs), newly developed porous crystalline materials constructed by metal clusters and organic linkers, are acknowledged to be relatively easy in this regard[5-9]. Because of their highly diversified structure, tailorable porosity, and tunable functionality, MOFs show great potential in various areas including adsorption[10-12], catalysis[13,14], chemical sensing[15,16], and electrochemistry[17,18]. Endowed with these fantastic features, MOFs are an ideal platform to customize functional materials on demand. Currently, various functional methods have been used in different kinds of MOF materials for a given system[19-21]. However, these functional approaches sometimes have poor versatility and are difficult to extend to other host MOFs or functional molecules[22]. In some cases, time- and resource-intensive processes are needed to find and design requisite host materials, functional parts, and their appropriate connection modes in each unit operation. Besides, it is also relatively difficult to impart some complex but useful functional molecules into MOF structures through direct postsynthetic substitution or sophisticated organic synthesis. Considering the variety and complexity of practical demands, a general strategy that allows the versatile and facile customization of MOFs according to a wide variety of applications is highly desirable yet remains a challenge to date.

To tackle the above-mentioned question, we here propose a "functional modular assembly" (FMA) strategy for customizing MOFs - a versatile conceptual approach that allows installing desired functional units into a host MOF material, opening up the possibility of assembling modular devices according to practical requirements. Such a novel strategy should possess the following features: (i) the functional module on the host MOF can be installed and switched freely, acting as a "plug and socket", and thus a proper functional unit can be inserted for a targeted application; (ii) to enrich modular diversity, the accessible functional molecules should be modularized as much as possible; (iii) the assembly step of installing functional modules onto host MOF should be accomplished in a simple manner, thereby facilitating target customization of MOFs in a facile and efficient way; and (iv) the host MOF material should be stable enough to be used in different conditions. In addition, as most MOFs are moisture sensitive and unstable in aqueous media, developing stable hydrophobic MOFs is necessary for practical applications[23,24].

To fulfill this goal, the proper connection mode between host material and modules is firstly needed. Considering the reversibility of coordination bonds in MOFs, postsynthetic substitution appears to be a reliable and simple approach to implementing installing and switching functional modules in MOFs. Moreover, combining different functional modules into one host MOF through multi-substitution may also open up the possibility of constructing multivariate MOFs (MTV-MOFs) for a target application. In this work, as a proof-of-concept experiment, we demonstrate that such a "functional modular assembly" strategy can be achieved on the highly robust MOF-808. This Zr-MOF was chosen as a host material for the following two reasons: (i) exceptional water/chemical stability; and (ii) the dangling formate groups on Zr_6 clusters are prone to be substituted by other ligands with carboxyl groups in a simple way, making it easy to

graft functional molecules/active fragments onto the host material. These interesting features of MOF-808 stimulate us to try to use the carboxyl group as a connector to assemble functional modular MOFs (FM-MOFs). Functional molecules with a carboxyl connector can be directly inserted into MOF-808 through single substitution. For functional molecules without a connector, we insert a pre-designed convertor and modules in a stepwise manner by tandem postsynthetic modification. That is, the convertor has two different terminals that can combine modules and MOF-808, respectively. Theoretically, a wide range of accessible functional molecules could be used as modules in the assembly process, thus generating practically numerous distinct new MOFs for functional targeting customization. To prove the feasibility of our strategy, several applications from completely different fields including adsorption, catalysis, fluorescent sensing, electrochemistry, and the control of surface wettability were selected as examples. Such tailor-made FM-MOFs exhibit excellent performance toward different target applications. Moreover, the functional units on our FM-MOFs can fully interconvert via a simple solvothermal method, readily implementing the installing and switching of modules in MOFs freely. Interestingly, we also found that two functional modules can be assembled into MOF-808 through partial conversion to construct multivariate FM-MOFs. Overall, this functional modular assembly strategy enables MOFs to achieve the goals of multi-modules, multi-objectives, switchable modules, and interfunctional coordination, providing a general and simple route for the rapid targeting customization of functional MOFs on demands.

RESULTS AND DISCUSSION

Customization of FM-MOFs by single substitution

A schematic illustration of the construction of FM-MOFs is shown in Scheme 1. Theoretically, in the assembly process, various desired functional modules could be imparted into the host framework to customize FM-MOFs according to arbitrary target applications. Thus, it is imperative to ensure that the various functional molecules can be modularized as much as possible. Considering that labile formate groups on MOF-808 are easy to be substituted, a carboxyl group can serve as a connector to impart functional molecules into MOF-808. To specify this concept, several applications including Hg^{2+} capture, Ag^{+} recovery, proton conductivity, detection of nitro explosives, and the control of surface wettability were taken as examples. We subsequently used thioglycollic acid (M1, M refers to module), propiolic acid (M2), oxalic acid (M3), pyrenecarboxylic acid (M4), and perfluorooctanoic acid (M5) to assemble series of FM-MOFs based on MOF-808 according to respective target applications [Figure 1 and Supplementary Figure 1]. Supplementary Figure 2 shows the PXRD patterns of MOF-808 and its functional derivatives. It is obvious that the related peaks of these assembled FM-MOFs are in good agreement with that of pristine MOF-808, confirming that the crystal structure of these materials remains intact after functional modules insertion. N_2 adsorption-desorption isotherms of FM-MOFs measured at 77 K display a typical I isotherm, suggesting the reservation of microporous features after introducing functional units into the framework, despite a decrease in their BET surface areas [Supplementary Figure 3]. The scanning electron microscopy (SEM) images demonstrate that our FM-MOFs possess octahedral morphology, with no apparent morphology change observed compared with MOF-808 [Supplementary Figure 4]. Individually, given that the thiolate ligand possesses a strong coordination ability to Hg^{2+}, thioglycollic acid (M1) was used as a functional modular to construct FM-MOF-1 for Hg^{2+} capture. The successful insertion of M1 into MOF-808 was also proved by Fourier transform infrared (FT-IR) spectroscopy, ^{1}H nuclear magnetic resonance (NMR) spectroscopy, and elemental analysis. The FT-IR spectra of FM-MOF-1 reveal that there is a new peak at 2564 cm^{-1} [Supplementary Figure 5], which can be attributed to the S-H stretching of free -SH groups. Supplementary Figure 6 shows the ^{1}H NMR spectra of FM-MOF-1 and MOF-808 after dissolving the samples in KOH/D_2O solution. Obviously, the peak intensity at δ = 8.3 ppm corresponding to the hydrogen of formate of FM-MOF-1 significantly decreased and a new peak at δ = 2.8 ppm for the hydrogen signal of $-CH_2-$ in M1 appeared, indicating that formate ligands on Zr_6 clusters were substituted by M1 molecules. All

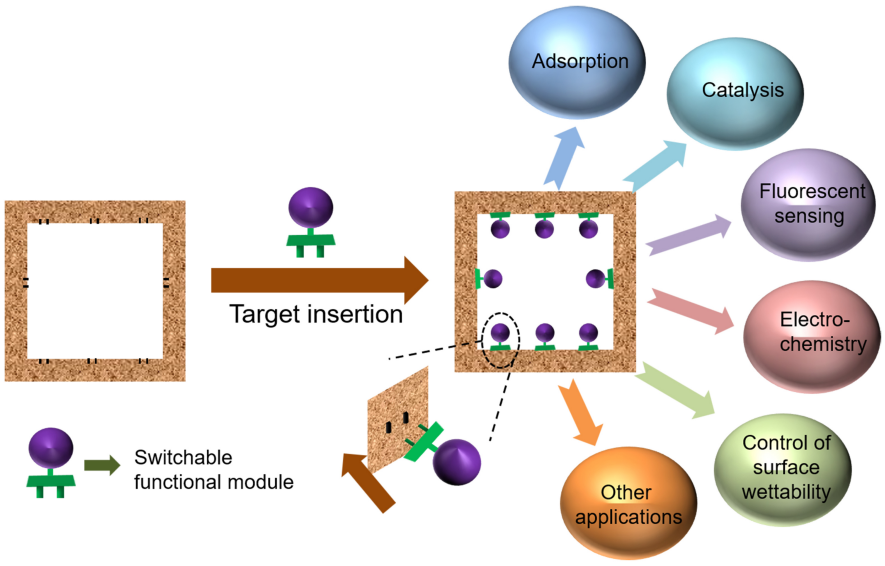

Scheme 1. Illustration of customization of FM-MOFs toward different applications.

these observations demonstrate that M1 was successfully inserted into the framework of MOF-808. To evaluate the effectiveness of FM-MOF-1 for Hg^{2+} capture, adsorption kinetics and isotherms were measured. As shown in Figure 1B and Supplementary Figure 7, an extremely quick process was observed for FM-MOF-1. Over 99% of Hg^{2+} was removed within 5 min. Supplementary Figure 8 shows the adsorption isotherms of FM-MOF-1 towards Hg^{2+}. By fitting with Langmuir model, the saturated Hg^{2+} removal capacity of FM-MOF-1 was estimated to be 758 mg g^{-1}, suggesting the great potential of FM-MOF-1 for Hg^{2+} capture. Similarly, considering the strong affinity of the terminal alkynyl group toward Ag^{+}, propiolic acid (M2) was selected as another functional module to assemble FM-MOF-2 for silver recovery. FT-IR and ^{1}H NMR spectra were used to demonstrate the successful insertion of M2 into the framework of MOF-808 [Supplementary Figures 9 and 10]. Supplementary Figure 11 shows the adsorption kinetics of FM-MOF-2 towards Ag^{+}; the removal efficiency increased sharply during the initial stage and then approached equilibrium after 2 h of contact. The adsorption isotherm revealed that FM-MOF-2 exhibits high silver uptake [Figure 1C]. By fitting with Langmuir model, the saturated Ag^{+} uptake capacity was calculated to be 806 mg g^{-1}, surpassing most reported porous materials [Supplementary Table 1][25-34]. This is also the first study of introducing alkynyl groups into the MOF framework for Ag^{+} recovery. Besides, to construct the proton-conducting MOF, we used oxalic acid as the functional module to assemble FM-MOF-3. The detailed characterizations are provided in the Supplementary Materials [Supplementary Figures 12-14]. Proton conductivities were then checked on a pressed plate at varying relative humidity (RH) from 33% to 100% at 298 K for FM-MOF-3. As shown in Supplementary Figure 15, all of the Nyquist plots display circular arcs at high frequencies. The proton conductivity of FM-MOF-3 increased with the elevated moisture [Figure 1D], suggesting water molecules play a vital role in the proton transportation of this MOF. Meanwhile, FM-MOF-3 exhibited a striking proton conductivity of 1.2 10^{-2} S cm^{-1} at 298 K and 100% RH, whereas the original MOF-808 displayed an inferior proton conductivity of 2.2 10^{-6} S cm^{-1} under the same condition [Supplementary Figure 16]. It should be noted that only a few MOFs featuring high proton conductivity over 10^{-2} S cm^{-1} have been reported[35-37]. Moreover, to achieve the goals of detecting nitro explosives and controlling surface wettability, conjugated pyrenecarboxylic acid (M4) and perfluorooctanoic acid (M5) were utilized as modules to construct FM-MOF-4 and FM-MOF-5, respectively. The related characterizations can be found in the Supplementary Materials [Supplementary Figures 17-20]. To investigate the explosive sensing ability of FM-MOF-4, fluorescence quenching titrations were conducted by

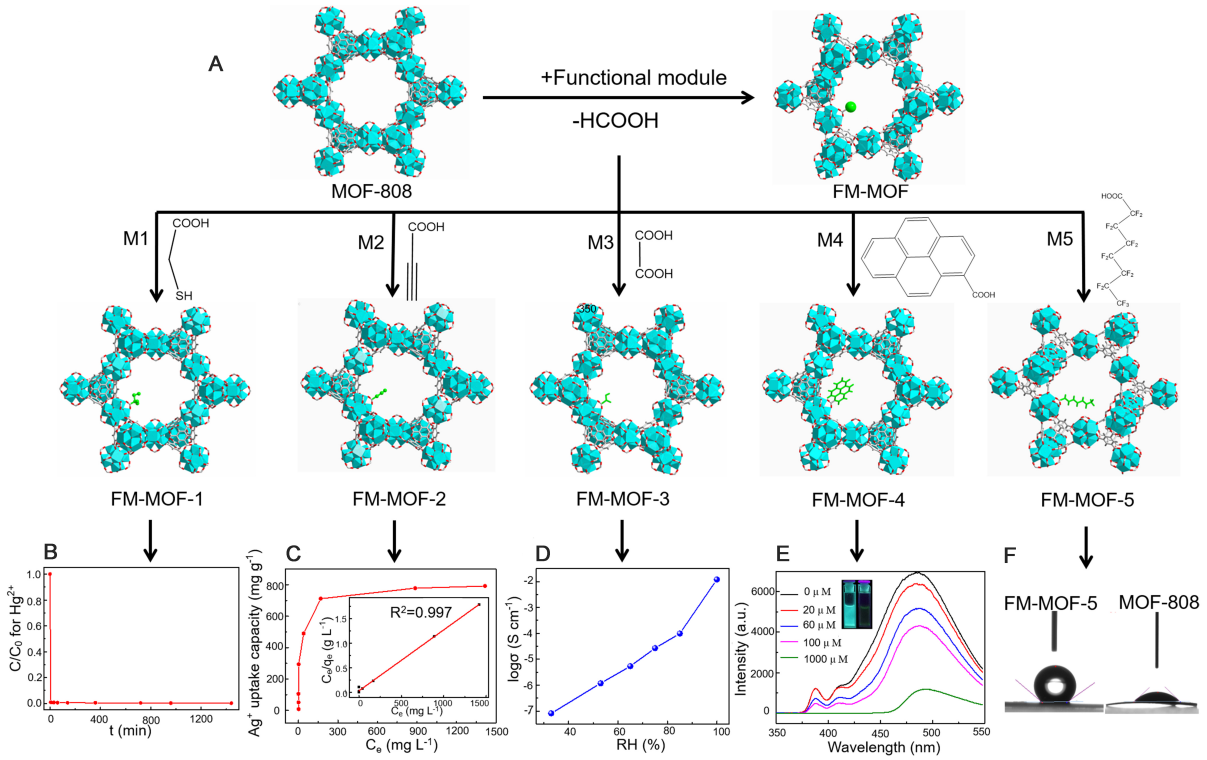

Figure 1. Customization of FM-MOFs through single substitution. (A) Schematic illustration of constructing FM-MOFs by functional modules with carboxyl connector. (B) Hg^{2+} adsorption kinetics of FM-MOF-1 at the initial concentration of 10 ppm. (C) Ag^{+} adsorption isotherm for FM-MOF-2. The inset shows the linear regression by fitting the experimental data with the Langmuir model. (D) Humidity dependence of the proton conductivities in FM-MOF-3 at room temperature. (E) The effect on the emission spectra of FM-MOF-4 dispersed in DMF upon incremental addition of a TNP solution (1 mM). The inset shows the original fluorescence and the decreased fluorescence upon the addition of TNP solution (1 mM). (F) Contact angle images of FM-MOF-5 and MOF-808.

the increasing amount of nitro aromatics. As shown in Figure 1E, fast and significant fluorescence quenching was observed with an increase in the amount of TNP (2,4,6-trinitrophenol). The fluorescence quenching could be discerned at a low concentration (0.5 μM; Supplementary Figure 21) and reached nearly 83% when the concentration of TNP increases to 1 mM. By contrast, other nitro compounds have little effect on the fluorescence intensity [Supplementary Figure 22]. These results demonstrate that FM-MOF-4 could selectively and sensitively detect TNP over other nitro explosives. On the other hand, the surface wettability of FM-MOF-5 and MOF-808 was also examined by contact angle measurements. As shown in Figure 1F, the contact angle of water on MOF-808 was estimated to be 37°, whereas FM-MOF-5 gave the water contact angle at as high as 142°. The surface character of MOF-808 transformed from hydrophilic to hydrophobic after M5 insertion into the framework, confirming the coating of perfluoroalkyl groups on the surface of material can dramatically enhance its hydrophobicity. This hydrophobic behavior of FM-MOF-5 was also illustrated by water vapor adsorption experiment: the water uptakes of MOF-808 reduced significantly after the incorporation of M5 [Supplementary Figure 23].

Customization of FM-MOFs through tandem postsynthetic modification

The above proof-of-concept experiments revealed that functional molecules with carboxyl groups can be used as modules to insert into MOF-808 directly according to numerous target applications. However, to expand the scope of our strategy, some useful functional molecules without carboxyl groups should also be modularized. To solve this problem, we installed a pre-designed convertor into MOF-808 before functional modules insertion through a tandem postsynthetic modification [Figure 2]. Such convertors should have

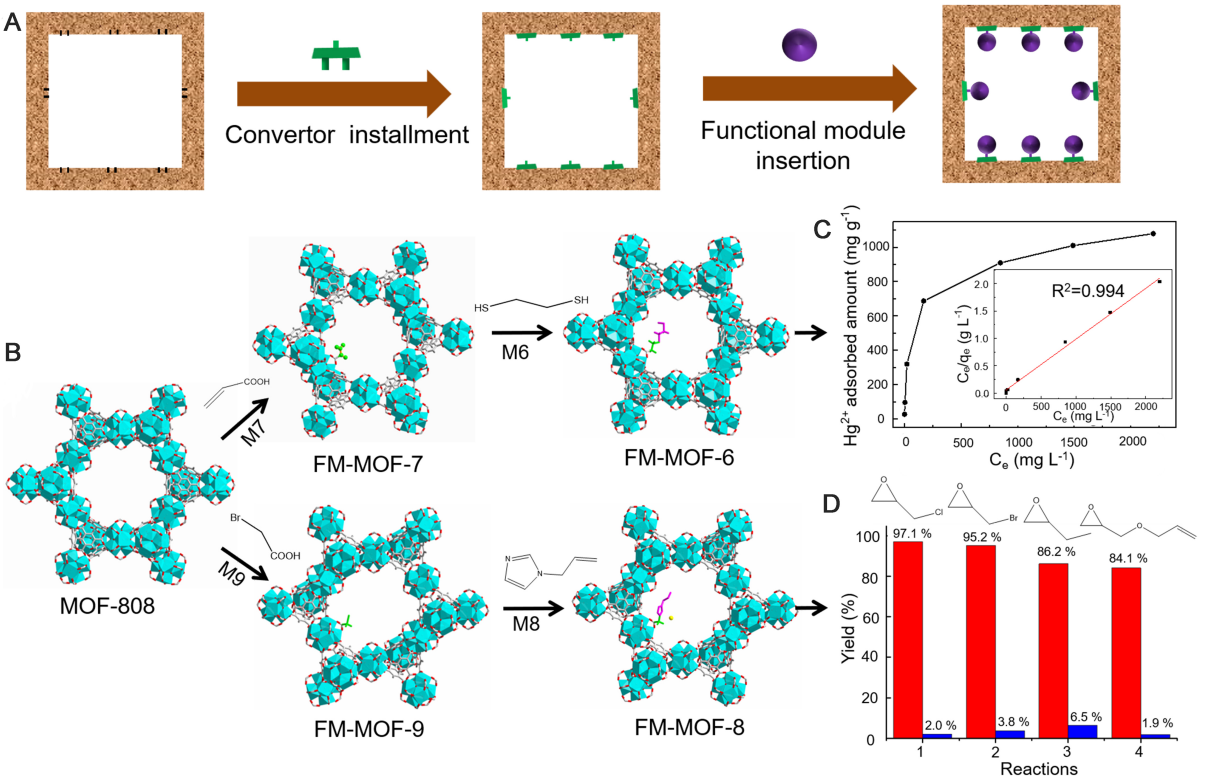

Figure 2. Customization of FM-MOFs through tandem postsynthetic modification. (A and B) Scheme illustration of FM-MOFs and their pore structures. (C) Hg^{2+} adsorption isotherm of FM-MOF-6. The inset shows the linear regression by fitting the experimental data with the Langmuir model. (D) Yields of various cyclic carbonates prepared from the cycloaddition of CO_2 with related epoxides catalyzed by FM-MOF-8 (red) and FM-MOF-9 (blue).

two terminals that can combine modules and the host framework, respectively. Here, the aforementioned Hg^{2+} capture and CO_2 conversion were taken as target applications to fully illustrate this. Firstly, we tried to use thioglycollic acid (M1) to construct FM-MOF-1 for mercury adsorption. Considering a functional unit with more chelating sites is needed to achieve higher Hg^{2+} uptake capacity, 1,2-ethanedithiol (M6) containing higher sulfur content yet without carboxyl group compared with M1 was adopted. To impart M6 on MOF-808, we chose propenoic acid (M7) as a convertor and inserted it into the host framework firstly to construct FM-MOF-7, where the accessible vinyl groups could allow for further chemical modifications. As shown in Supplementary Figures 24-28, FM-MOF-7 was characterized by PXRD, N_2 adsorption, SEM, FT-IR, and ^{1}H NMR. FT-IR spectra reveal the appearance of a new characteristic peak at 1639 cm^{-1} compared with MOF-808, which can be attributed to the C=C stretching band of vinyl groups [Supplementary Figure 27]. ^{1}H NMR spectra demonstrate that the peak at 8.3 ppm assigned to the formate groups disappeared and several strong peaks around 5.0-7.0 ppm corresponding to the vinyl groups emerged, indicating the successful insertion of M7 into MOF-808 [Supplementary Figure 28]. FM-MOF-7 was then treated with 1,2-ethanedithiol (M6) to obtain FM-MOF-6 through the thiol-ene "click" reaction between thiol compounds and the vinyl groups in FM-MOF-7. The resulting material was also carefully characterized by PXRD, N_2 adsorption, FT-IR, SEM, and NMR [Supplementary Figures 29-33]. Compared with FM-MOF-7, FT-IR spectra of FM-MOF-6 show a new peak at 2555 cm^{-1} despite the absence of the band at 1639 cm^{-1}, indicating the elimination of vinyl groups and the appearance of free-standing thiol group after modification [Supplementary Figure 32]. The thio-ene transformation was also confirmed by the disappearance of the peaks around 5.0-7.0 ppm corresponding to the hydrogen signals of vinyl groups in the ^{1}H NMR spectrum of FM-MOF-6 and the concomitant emergence of new peaks around 2.0 and 3.0

ppm attributed to the different hydrogen of -CH_2- in M6 [Supplementary Figure 33]. To assess the overall capacity of FM-MOF-6 towards Hg^{2+}, the adsorption isotherm was then measured. As shown in Figure 2C, FM-MOF-6 displayed extremely high Hg^{2+} uptake. By fitting with Langmuir model, the saturated adsorption capacity of FM-MOF-6 for Hg^{2+} was determined to be 1077 mg g^{-1}, which is about 1.4 times higher than that of FM-MOF-1, surpassing various MOF adsorbents Supplementary Table 2[38-48]. In addition, we also investigated the adsorption kinetics of FM-MOF-6 toward Hg^{2+}. As shown in Supplementary Figure 34, a quick purification process was observed. The removal efficiency displayed a steep profile at the initial stage and then tended to equilibrium with about 99.84% of Hg^{2+} ions being removed. The excellent performance of FM-MOF-6 in mercury capture can be traced to the strong binding interactions between the Hg and sulfur species in FM-MOF-6, as evidenced by the enlarged S 2p binding energy of XPS analysis and the absence of S-H stretching mode in FT-IR spectra after Hg^{2+} adsorption [Supplementary Figures 35-37]. These results demonstrate the superiority of the utilization of FM-MOF-6 as a promising candidate for mercury capture from aqueous solutions.

On the other hand, the cycloaddition of CO_2 with epoxides into cyclic carbonates is an attractive strategy for addressing anthropogenic CO_2 emission issues, and imidazole-based functional molecules are regarded as efficient catalysts for this purpose. Considering the issues of homogeneous catalysts in product purification and catalyst recycling, it is advisable to graft imidazole-based functional molecules onto host materials for use as heterogeneous catalysts. Here, we chose 1-allylimidazole (M8) as a functional module to construct FM-MOF-8. Because of the absence of carboxylic connector in M8, a suitable convertor was needed. Therefore, bromoacetic acid (M9), which contains both a carboxylic connector and an accessible bromomethyl group for further chemical modification, was selected to assemble FM-MOF-9 first. The detailed characterizations are provided in Supplementary Figures 38-42. FM-MOF-9 was then treated with 1-allylimidazole (M8) through a tandem postsynthetic modification to obtain FM-MOF-8, as characterized by PXRD, N_2 adsorption, SEM, FT-IR, and NMR [Supplementary Figures 43-47]. Interestingly, the two incorporated modules of M8 and M9 in FM-MOF-8 combined together to form an imidazolium-based ionic liquid (IL) unit. Because of the proper distribution of formate groups in MOF-808, theoretically, such IL unit in FM-MOF-8 would also disperse uniformly within the pore, thus avoiding agglomeration and providing more accessible catalytic sites compared to the conventional dipping method. To evaluate the effectiveness of FM-MOF-9 as a catalyst, experiments were carried out. As shown in Figure 2D, the reaction yields catalyzed by FM-MOF-8 from related epoxides were determined to be 97.1% for epichlorohydrin, 95.2% for epibromohydrin, 86.2% for 1,2-epoxybutane, and 84.1% for allyl glycidyl ether, indicating that FM-MOF-8 exhibited a highly efficient catalytic performance for a variety of epoxides. It should be noted that the good performance of FM-MOF-8 was achieved without using any co-catalysts, whereas most reported MOF catalysts employ other substances, such as TBAB, to improve activity, which is considered uneconomical and complicated[49]. In contrast, FM-MOF-9 showed an extremely low activity, with a yield of < 10% under similar conditions, manifesting that the grafted M8 played a key role during the catalytic process. The above two proof-of-concept experiments fully demonstrated the reliability of this tandem postsynthetic modification for inserting functional modules without a carboxyl connector into MOF-808, which greatly expands the scope of FM-MOFs for functional targeting customization.

Switching modules on FM-MOFs

Another important aspect to consider is whether the functional modules on FM-MOFs could be freely switched in a simple manner, which allows for changing user-defined units in accordance with different needs, thereby affording matrix recycling and cost saving. The mutual transformation among FM-MOF-2, FM-MOF-7, and FM-MOF-9 was taken as a representative sample to confirm this [Figure 3]. These FM-MOFs were added into the solution containing the corresponding functional module, and the detailed experiments can be found in the Supplementary Materials. This conversion process was repeated several

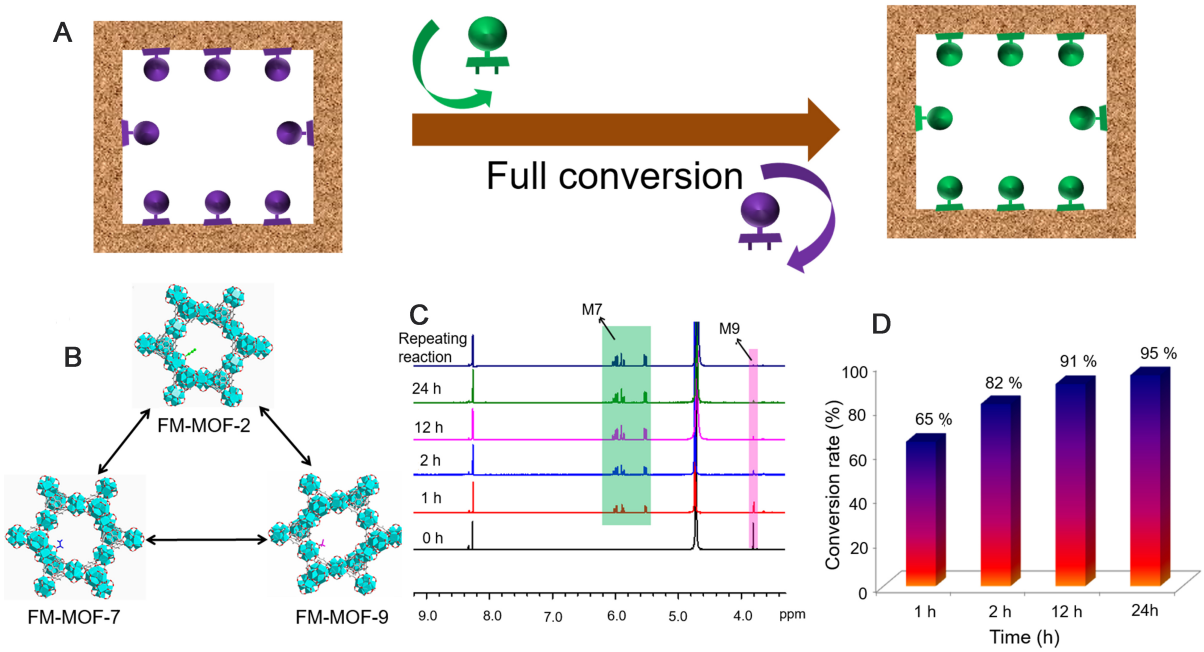

Figure 3. Full conversion process among FM-MOFs: (A and B) scheme illustration of mutual transformation among FM-MOFs and the associated pore structures of FM-MOF-2, FM-MOF-7, and FM-MOF-9; (C) the conversion process characterized by ^{1}H NMR spectra; and (D) the conversion rate from FM-MOF-9 to FM-MOF-7 with the increase of time.

times, and the as-transformed FM-MOFs were determined by ^{1}H NMR analysis. As shown in Supplementary Figures 48-53, for all three FM-MOFs, the signals of the original functional module disappeared, whereas the peaks attributed to the new unit emerged, demonstrating full switching of functional modules on MOF-808. Besides, PXRD measurements indicate no apparent loss of crystallinity during the conversion process [Supplementary Figures 54-59]. To further illustrate this, we also symmetrically investigated the conversion process from FM-MOF-9 to FM-MOF-7 with the increase of time. As shown in Figure 3C and D, the conservation rate reached 65% in the initial 1 h and steadily increased over time. After 24 h of reaction, the ^{1}H NMR spectrum reveals that δ at 3.8 ppm corresponding to the hydrogen signals of -CH_2- in M9 significantly decreased, whereas several new peaks around 5-7 ppm attributed to the vinyl group in M7 enhanced dramatically, achieving a high conservation of 95%. The peak of M9 further reduced when we repeated this conservation process several times, demonstrating essentially full conversion from FM-MOF-9 to FM-MOF-7.

Interestingly, we found that two functional modules could coexist in one host matrix during the switching process, which would form multivariate MOFs (MTV-MOFs) via partial conversion [Figure 4]. For full illustration, Hg^{2+} detection was selected as target application. We combined a mercury capture module and fluorophore moiety into MOF-808 through partial conservation and supposed that the resulting MTV-MOF would show improved performance in mercury detection. As such, the aforementioned FM-MOF-1 was immersed in DMF solution containing M4 for a period of time to obtain FM-MOF-1-4 (see Supplementary Figures 60-62). Compared to FM-MOF-1, the ^{1}H NMR spectra of this MTV-MOF reveal that δ at 2.8 ppm corresponding to M1 decreased and new peaks assigned to the hydrogen signals of pyrene in M4 emerged [Figure 4C]. The relevant signals of M1 in FM-MOF-1 and FM-MOF-1-4 were also integrated against that of the BTC ligand, resulting in peak ratios of 6:7 and 6:2, respectively, demonstrating that 71% of M1 was substituted by M4 during module switching process [Supplementary Figures 63 and 64]. FM-MOF-1-4 was then used to sense a trace quantity of Hg^{2+} in aqueous solutions. As shown in Figure 4D, obvious

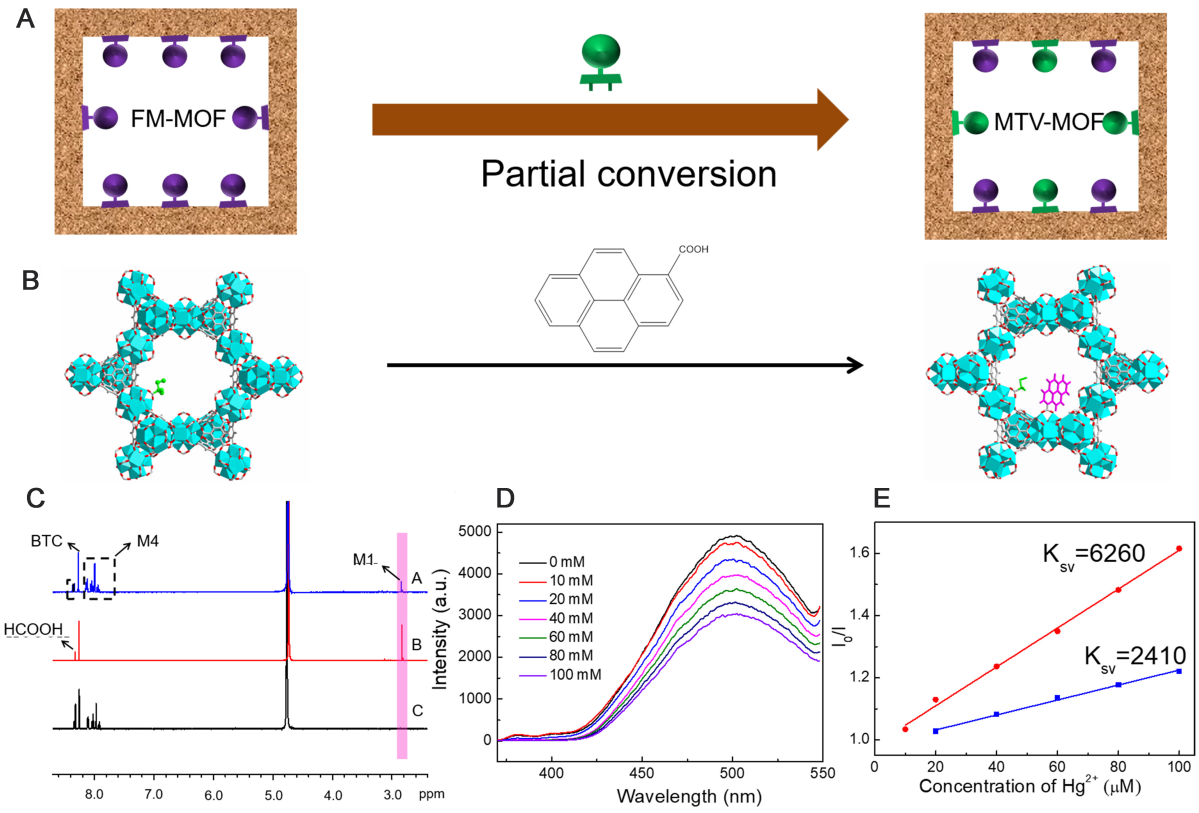

Figure 4. Partial conversion process among FM-MOFs: (A) scheme illustration of constructing MTV-MOF through a partial conversion process; (B) constructing FM-MOF-1-4 from FM-MOF-1; (C) ^{1}H NMR spectra of (A) FM-MOF-1-4, (B) FM-MOF-1, and (C) FM-MOF-4 in D_2O/KOH solution; (D) effect on the emission spectra of FM-MOF-1-4 with different concentration of Hg^{2+} in aqueous solution; and (E) Stern-Volmer plots of Hg^{2+} in aqueous solution for FM-MOF-1-4 (red) and FM-MOF-4 (blue).

fluorescence quenching was observed as the concentration of Hg^{2+} increased from 10 to 100 μM, specially, the quenching effect of Hg^{2+} was quantified by the Stern-Volmer equation ($I_0/I = 1 + K_{sv}[M]$), where I_0 and I are emission intensity of MOF material before and after reaction with Hg^{2+}, K_{sv} is the Stern-Volmer quenching effect constant of Hg^{2+}, and [M] is the concentration of Hg^{2+}. As shown in Figure 4E, FM-MOF-1-4 showed a distinguishable K_{sv} value for Hg^{2+} at 6260 M^{-1}, which is 2.6 times higher than that of FM-MOF-4 at 2410 M^{-1}. It is worth noting that FM-MOF-1 exhibited very weak fluorescence, and no visible quenching effect was observed towards Hg^{2+}. With M4 anchored in the pores, the thiol group within MOF and the fluorophore part of pyrene can cooperatively interact to significantly improve sensing performance. Specifically, the thiol groups of M1 in MOF captured traces of Hg^{2+}, and then the fluorophore pyrene of M4, which is in close proximity, responded to mercury ions. This process allows two functional modules to work in a cooperative manner. The above representative sample, therefore, demonstrates the feasibility of constructing MTV-MOF via partial conversion, which may further enhance the performance of MOFs. In principle, two arbitrary functional modules can exist in one host MOFs, thus constructing numerous of MTV-MOFs for target applications.

CONCLUSION

We propose a versatile "functional modular assembly" strategy for customizing MOFs, which allows installing the desired functional unit into a host material, and the unit can be switched flexibly according to different requirements. Functional molecules with connectors could be used as modules to insert into MOF structures through single substitution directly. To enrich modular diversity, molecules without connectors

could also be modularized by inserting pre-designed convertors into MOFs ahead through tandem postsynthetic modifications. Therefore, a wide range of available functional molecules, both with and without connectors, could be modularized during such an assembly process. Thus, a series of tailor-made FM-MOFs were generated and showed excellent performance toward entirely different fields, covering adsorption, catalysis, fluorescent sensing, electrochemistry, and the control of surface wettability. Moreover, the functional units on our FM-MOFs can be freely switched via full interconversion. Interestingly, we also found that two functional modules could coexist in one host matrix through partial conversion, opening up the possibility to construct multivariate MOFs (MTV-MOFs). Our strategy, therefore, provides a versatile and simple route for the rapid targeting customization of functional MOFs according to diverse applications, achieving the goals of multi-modules, multi-objectives, switchable units, and interfunctional cooperation for FM-MOFs.

DECLARATIONS

Authors' contributions

Planned the study, analyzed the data and prepare the manuscript: Peng Y, Tan Q, Huang H
Performed manuscript correcting: Kang X, Zhu Q, Zhong C, Han B

Availability of data and materials

The experimental data and details are available from the Supplementary Materials.

Financial support and sponsorship

This work is supported by Beijing Natural Science Foundation (2222043) and National Natural Science Foundation of China (21978212).

Conflict of interest

All authors declared that there are no conflicts of interest.

Ethical approval and consent to participate

Not applicable.

Consent for publication

Not applicable.

REFERENCES

1. Slater AG, Cooper AI. Porous materials. Function-led design of new porous materials. *Science* 2015;348:aaa8075. DOI PubMed
2. Kitagawa S. Future porous materials. *Acc Chem Res* 2017;50:514-6. DOI PubMed
3. Wu J, Xu F, Li S, et al. Porous polymers as multifunctional material platforms toward task-specific applications. *Adv Mater* 2019;31:e1802922. DOI PubMed
4. Siegelman RL, Kim EJ, Long JR. Porous materials for carbon dioxide separations. *Nat Mater* 2021;20:1060-72. DOI PubMed
5. Kirchon A, Feng L, Drake HF, Joseph EA, Zhou HC. From fundamentals to applications: a toolbox for robust and multifunctional MOF materials. *Chem Soc Rev* 2018;47:8611-38. DOI PubMed
6. Cui Y, Li B, He H, Zhou W, Chen B, Qian G. Metal-organic frameworks as platforms for functional materials. *Acc Chem Res* 2016;49:483-93. DOI PubMed
7. Li B, Chrzanowski M, Zhang Y, Ma S. Applications of metal-organic frameworks featuring multi-functional sites. *Coordin Chem Rev* 2016;307:106-29. DOI
8. Deng H, Doonan CJ, Furukawa H, et al. Multiple functional groups of varying ratios in metal-organic frameworks. *Science* 2010;327:846-50. DOI PubMed

9. Han Y, Li JR, Xie Y, Guo G. Substitution reactions in metal-organic frameworks and metal-organic polyhedra. *Chem Soc Rev* 2014;43:5952-81. DOI PubMed
10. Li J, Wang X, Zhao G, et al. Metal-organic framework-based materials: superior adsorbents for the capture of toxic and radioactive metal ions. *Chem Soc Rev* 2018;47:2322-56. DOI PubMed
11. Peng Y, Huang H, Zhang Y, et al. A versatile MOF-based trap for heavy metal ion capture and dispersion. *Nat Commun* 2018;9:187. DOI PubMed PMC
12. Peng Y, Zhang Y, Tan Q, Huang H. Bioinspired construction of uranium ion trap with abundant phosphate functional groups. *ACS Appl Mater Interfaces* 2021;13:27049-56. DOI PubMed
13. Shen Y, Pan T, Wang L, Ren Z, Zhang W, Huo F. Programmable logic in metal-organic frameworks for catalysis. *Adv Mater* 2021;33:e2007442. DOI PubMed
14. Newar R, Akhtar N, Antil N, et al. Amino acid-functionalized metal-organic frameworks for asymmetric base-metal catalysis. *Angew Chem Int Ed Engl* 2021;60:10964-70. DOI PubMed
15. Cui Y, Yue Y, Qian G, Chen B. Luminescent functional metal-organic frameworks. *Chem Rev* 2012;112:1126-62. DOI PubMed
16. Wang B, Lv XL, Feng D, et al. Highly stable Zr(IV)-based metal-organic frameworks for the detection and removal of antibiotics and organic explosives in water. *J Am Chem Soc* 2016;138:6204-16. DOI PubMed
17. Li H, Li C, Wang Y, et al. Selenium confined in ZIF-8 derived porous carbon@MWCNTs 3D networks: tailoring reaction kinetics for high performance lithium-selenium batteries. *Chem Synth* 2022;2:8. DOI
18. Kang X, Wang B, Hu K, et al. Quantitative electro-reduction of CO_2 to liquid fuel over electro-synthesized metal-organic frameworks. *J Am Chem Soc* 2020;142:17384-92. DOI PubMed PMC
19. Li N, Chang Z, Zhong M, et al. Functionalizing MOF with redox-active tetrazine moiety for improving the performance as cathode of Li-O_2 batteries. *CCS Chem* 2021;3:1297-305. DOI
20. Cho W, Lee HJ, Choi G, Choi S, Oh M. Dual changes in conformation and optical properties of fluorophores within a metal-organic framework during framework construction and associated sensing event. *J Am Chem Soc* 2014;136:12201-4. DOI PubMed
21. Deria P, Bury W, Hupp JT, Farha OK. Versatile functionalization of the NU-1000 platform by solvent-assisted ligand incorporation. *Chem Commun (Camb)* 2014;50:1965-8. DOI PubMed
22. Zhu W, Xiang G, Shang J, et al. Versatile surface functionalization of metal-organic frameworks through direct metal coordination with a phenolic lipid enables diverse applications. *Adv Funct Mater* 2018;28:1705274. DOI
23. Jayaramulu K, Geyer F, Schneemann A, et al. Hydrophobic metal-organic frameworks. *Adv Mater* 2019;31:e1900820. DOI PubMed
24. Mukherjee S, Datta K, Fischer RA. Hydrophobicity: a key factor en route to applications of metal-organic frameworks. *Trends in Chemistry* 2021;3:911-25. DOI
25. Hou H, Yu D, Hu G. Preparation and properties of ion-imprinted hollow particles for the selective adsorption of silver ions. *Langmuir* 2015;31:1376-84. DOI PubMed
26. Yao Y, Gao B, Wu F, Zhang C, Yang L. Engineered biochar from biofuel residue: characterization and its silver removal potential. *ACS Appl Mater Interfaces* 2015;7:10634-40. DOI PubMed
27. Zhang M, Zhang Y, Helleur R. Selective adsorption of Ag^+ by ion-imprinted O-carboxymethyl chitosan beads grafted with thiourea-glutaraldehyde. *Chemical Engineering Journal* 2015;264:56-65. DOI
28. Wang L, Wang K, Huang R, Qin Z, Su Y, Tong S. Hierarchically flower-like WS_2 microcrystals for capture and recovery of Au (III), Ag (I) and Pd (II). *Chemosphere* 2020;252:126578. DOI PubMed
29. Pan X, Fu L, Wang H, Xue Y, Zu J. Synthesis of novel sulfydryl-functionalized chelating adsorbent and its application for selective adsorption of Ag(I) under high acid. *Separation and Purification Technology* 2021;271:118778. DOI
30. Fard Z, Malliakas CD, Mertz JL, Kanatzidis MG. Direct extraction of Ag^+ and Hg^{2+} from cyanide complexes and mode of binding by the layered $K_2MgSn_2S_6$ (KMS-2). *Chem Mater* 2015;27:1925-8. DOI
31. Ma L, Wang Q, Islam SM, Liu Y, Ma S, Kanatzidis MG. Highly Selective and Efficient Removal of Heavy Metals by Layered Double Hydroxide Intercalated with the MoS4(2-) Ion. *J Am Chem Soc* 2016;138:2858-66. DOI PubMed
32. Zhou Y, Gao B, Zimmerman AR, Cao X. Biochar-supported zerovalent iron reclaims silver from aqueous solution to form antimicrobial nanocomposite. *Chemosphere* 2014;117:801-5. DOI PubMed
33. Asiabi H, Yamini Y, Shamsayei M, Molaei K, Shamsipur M. Functionalized layered double hydroxide with nitrogen and sulfur co-decorated carbondots for highly selective and efficient removal of soft Hg^{2+} and Ag^+ ions. *J Hazard Mater* 2018;357:217-25. DOI PubMed
34. Das R, Giri S, King Abia AL, Dhonge B, Maity A. Removal of noble metal ions (Ag^+) by mercapto group-containing polypyrrole matrix and reusability of its waste material in environmental applications. *ACS Sustainable Chem Eng* 2017;5:2711-24. DOI
35. Wu H, Yang F, Lv X, et al. A stable porphyrinic metal-organic framework pore-functionalized by high-density carboxylic groups for proton conduction. *J Mater Chem A* 2017;5:14525-9. DOI
36. Xue WL, Deng WH, Chen H, et al. MOF-directed synthesis of crystalline ionic liquids with enhanced proton conduction. *Angew Chem Int Ed Engl* 2021;60:1290-7. DOI PubMed
37. Sharma A, Lim J, Jeong S, et al. Superprotonic conductivity of MOF-808 achieved by controlling the binding mode of grafted sulfamate. *Angew Chem Int Ed Engl* 2021;60:14334-8. DOI PubMed
38. Yee KK, Reimer N, Liu J, et al. Effective mercury sorption by thiol-laced metal-organic frameworks: in strong acid and the vapor phase. *J Am Chem Soc* 2013;135:7795-8. DOI PubMed

39. Hou YL, Yee KK, Wong YL, et al. Metalation triggers single crystalline order in a porous solid. *J Am Chem Soc* 2016;138:14852-5. DOI PubMed
40. Luo F, Chen JL, Dang LL, et al. High-performance Hg^{2+} removal from ultra-low-concentration aqueous solution using both acylamide- and hydroxyl-functionalized metal-organic framework. *J Mater Chem A* 2015;3:9616-20. DOI
41. Zhao M, Huang Z, Wang S, Zhang L, Zhou Y. Design of l-cysteine functionalized UiO-66 MOFs for selective adsorption of Hg(II) in aqueous medium. *ACS Appl Mater Interfaces* 2019;11:46973-83. DOI PubMed
42. Shi M, Lin D, Huang R, Qi W, Su R, He Z. Construction of a mercapto-functionalized Zr-MOF/melamine sponge composite for the efficient removal of oils and heavy metal ions from water. *Ind Eng Chem Res* 2020;59:13220-7. DOI
43. Liang L, Chen Q, Jiang F, et al. In situ large-scale construction of sulfur-functionalized metal-organic framework and its efficient removal of Hg(ii) from water. *J Mater Chem A* 2016;4:15370-4. DOI
44. Liang L, Liu L, Jiang F, et al. Incorporation of In_2S_3 nanoparticles into a metal-organic framework for ultrafast removal of hg from water. *Inorg Chem* 2018;57:4891-7. DOI PubMed
45. Jiang SY, He WW, Li SL, Su ZM, Lan YQ. Introduction of molecular building blocks to improve the stability of metal-organic frameworks for efficient mercury removal. *Inorg Chem* 2018;57:6118-23. DOI PubMed
46. Li J, Duan Q, Wu Z, et al. Few-layered metal-organic framework nanosheets as a highly selective and efficient scavenger for heavy metal pollution treatment. *Chemical Engineering Journal* 2020;383:123189. DOI
47. Mon M, Lloret F, Ferrando-soria J, Martí-gastaldo C, Armentano D, Pardo E. Selective and efficient removal of mercury from aqueous media with the highly flexible arms of a BioMOF. *Angew Chem* 2016;128:11333-8. DOI PubMed
48. Fu K, Liu X, Lv C, et al. Superselective Hg(II) removal from water using a thiol-laced MOF-based sponge monolith: performance and mechanism. *Environ Sci Technol* 2022;56:2677-88. DOI PubMed
49. Nguyen PTK, Nguyen HTD, Nguyen HN, et al. New metal-organic frameworks for chemical fixation of CO_2. *ACS Appl Mater Interfaces* 2018;10:733-44. DOI PubMed

Hongliang Huang

Hongliang Huang received his B.S. degree and Ph.D. degree from Beijing University of Chemical Technology in 2009 and 2014, respectively. He joined the group of Prof. Chongli Zhong and worked as a postdoctoral fellow from 2014 to 2016. He has worked as a associate professor in Tiangong University since 2017. His research interests mainly focus on the design and synthesis of new porous materials (such as metal-organic frameworks and covalent organic frameworks) and their applications in gas separation, water treatment and catalysis.

Xinchen Kang

Xinchen Kang received his B.S. degree from Shandong University in 2011 and Ph.D. degree from Institute of Chemistry, Chinese Academy of Sciences (ICCAS) since 2016. He worked as a Royal Society research fellow in the University of Manchester from 2017 to 2020. He has worked as a professor in the group of Prof. Buxing Han in ICCAS since Jun, 2021. He is youth editorial board of *Chemical Synthesis*, youth editorial board of *Acta Physico-Chimica Sinica* and guest editor of *Symmetry*. His research fields include solution chemistry, materials chemistry and catalysis.

Buxing Han

Buxing Han received his Ph.D. degree in Physical Chemistry at Institute of Chemistry, CAS in 1988, and did postdoctoral research in Chemical Engineering at the University of Saskatchewan, Canada from 1989 to 1991. He was associate professor at Institute of Chemistry, CAS during 1991-1993, and has been a professor at the Institute since 1993. He is now the professor at Institute of Chemistry, Chinese Academy of Sciences (CAS); Academician of Chinese Academy of Sciences; Fellow of the Academy of Sciences for the Developing World (TWAS); Fellow of Royal Society of Chemistry. His research interests include physicochemical properties of green solvent systems and applications of green solvents in green chemistry, especially transformation of CO_2, biomass, and waste plastics. He is a Chief Scientist of China Innovation Think Tank; Secretary of Interdivisional Committee on Green Chemistry for Sustainable Development, (ICGCSD), Union of Pure and Applied Chemistry (IUPAC); Chairman of Green Chemistry Division, Chinese Chemical Society; President of Beijing Energy and Environment Society; Vice President of Energy Technology Industry Association of China; Former Chairman of Subcommittee on Green Chemistry of IUPAC, former Titular Member of Division III of IUPAC, and former Chairman of Thermodynamics and Thermal Analysis Committee, Chinese Chemical Society. He is an Editor-in-Chief of *The Innovation*, Associate Editors of *Green Chem.*, Associate Editor of *Chinese Sci. Bulletin*, Associate Editor of *Acta Physico-Chimica Sinica*, Associate Editor of *Chemical Journal of Chinese Universities*.

Yaguang Peng

Yaguang Peng joined the group of Prof. Chongli Zhong in Beijing University of Chemical Technology from 2013 and received his Ph.D. degree in chemical engineering and technology in 2019. He worked as a postdoctoral fellow in the group of Prof. Yadong Li in the department of chemistry, Tsinghua University from 2019 to 2021. He currently worked as a postdoctoral fellow in the group of Prof. Buxing Han and Prof. Xinchen Kang in ICCAS. His research interests mainly focus on the design and synthesis of metal-organic frameworks and their applications in adsorption, separation and CO_2 electro-reduction.